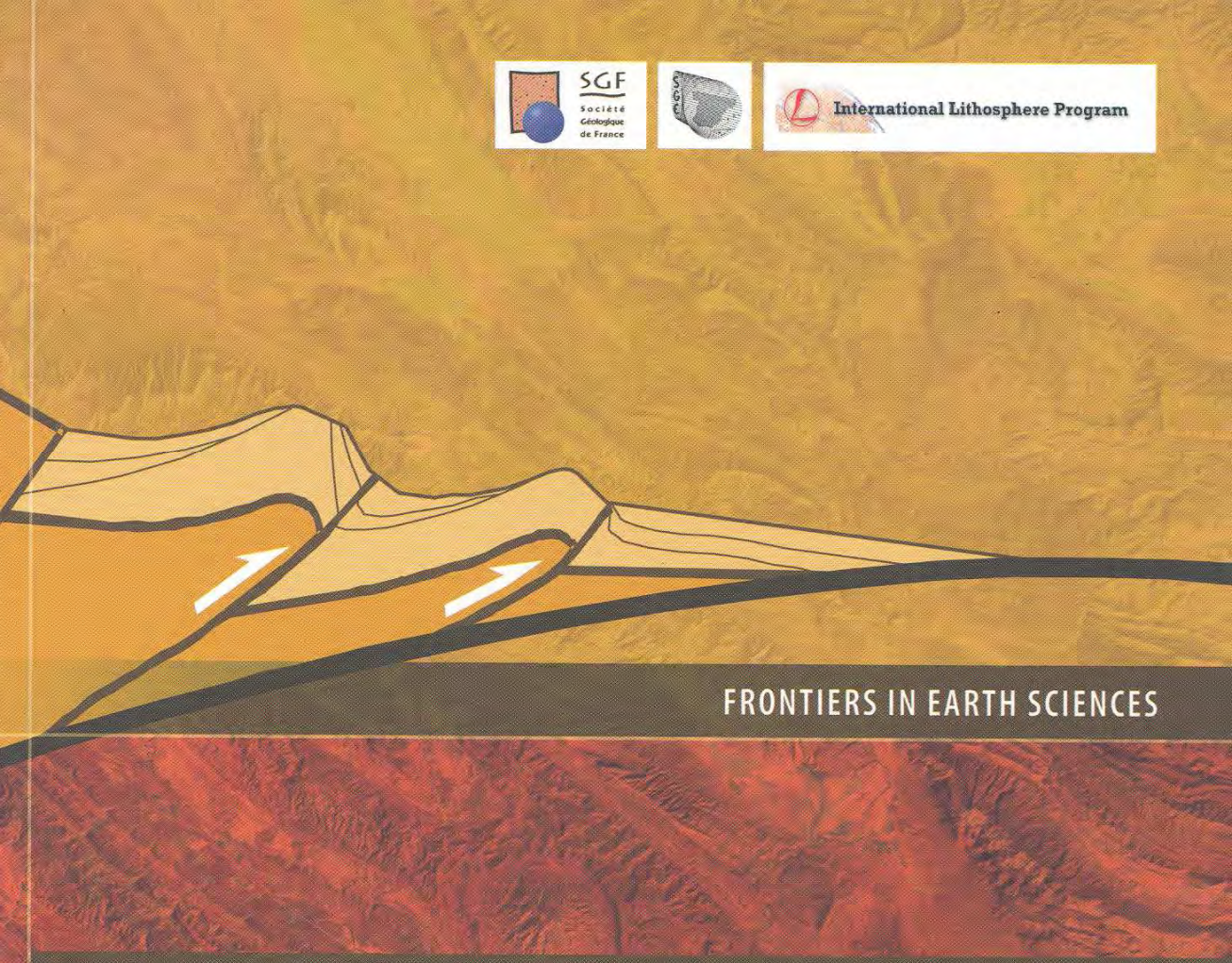

FRONTIERS IN EARTH SCIENCES

O. Lacombe · J. Lavé · F. Roure · J. Vergés (Eds.)

Thrust Belts and Foreland Basins

From Fold Kinematics to Hydrocarbon Systems

Springer

Meso-Cenozoic Evolution of Mountain Range - Intramontane Basin Systems in the Southern Siberian Altai Mountains by Apatite Fission-Track Thermochronology

Johan De Grave · Michael M. Buslov · Peter Van den haute · Boris Dehandschutter · Damien Delvaux

Abstract. The Altai Mountains form the northern part of the Cenozoic Central Asian intracontinental orogenic system that developed as a far-field effect of ongoing India-Eurasia convergence. Our study focuses on the southern Siberian Altai Mountains where basement rocks for apatite fission-track (AFT) analysis were sampled. These rocks are mainly Paleozoic granitoids that currently outcrop in several high mountain ranges along reactivated transpressive Paleozoic fault zones. These ranges are in most cases thrust systems adjacent to lacustrine intramontane basins. We present AFT results from the Chuya and Kurai ranges (3 samples) that are thrust over Late Cenozoic sediments of the Chuya-Kurai Basin and from the Shapshal range (4 samples) east of the Dzhulukul Basin. In addition, 5 samples were collected along a transect west of aforementioned study areas in the low-elevation areas of the Siberian Altai or Gorny Altai. Apparent AFT ages were found to be Mesozoic (roughly ranging between 180 and 80 Ma) and AFT length distributions show signs of thermal track fading (mean track lengths vary between 11.3 and 14.1 µm). AFT age and length data were modelled and thermal histories for the different sample sites reconstructed. These yield a two- to three-stage evolution: Late Jurassic-Cretaceous rapid basement cooling, a prolonged period of Late Cretaceous to Paleogene-Neogene stability, and a possible Late Cenozoic cooling to ambient temperatures.

Keywords. Apatite fission-track thermochronology, Siberia, Altai, intracontinental tectonics

1 Introduction

The Altai Mountains are an active intracontinental mountain belt located in the border zone of South Siberia (Russia–Gorny Altai Autonomous Republic), Kazakhstan, Mongolia, and China (Fig. 1). This paper deals with the southern Siberian Altai Mountains, and in particular with the areas around the Chuya-Kurai and Dzhulukul basins (Fig. 1). The Altai Mountains are part of a vast area in Central Asia and Siberia that is subjected to Late Cenozoic and active, mainly transpressive intracontinental deformation. This area includes the Tien Shan, Altai, Sayan, and Baikal rift zone as major constituents. These mountain belts alternate with large, undeformed basins, e.g., Tarim, Junggar, the Mongolian depressions (Great Lakes Depression) (Fig. 1). We refer to this region as the Central Asian Deformation Zone (CADZ), the world's largest intracontinental active orogenic system. Other terminologies have been used to delineate this area. In Russian literature, the area is often called the Ural-Mongolian fold belt, corresponding to the Altaids defined by Şengör et al. (1993). The driving forces for this regional deformation are generated by ongoing indentation of the Indian plate into Eurasia and possibly the Pacific Ocean subduction under eastern Asia (Molnar and Tapponnier, 1975; Tapponnier and Molnar, 1979; Avouac and Tapponnier, 1993). Strain accumulated in the convergence zone is partitioned to Eurasia's continental interior along an intricate pre-existing structural network associated with Central Asian Paleozoic basement and accretion tectonics. Reactivation is hence mostly basement controlled (Dobretsov et al., 1995b; Allen and Vincent, 1997) and involves primarily the easier to deform sutures and mobile belts between rigid units that compose the complex blocky tectonic CADZ collage. The Altai Mountains between the Paleozoic Altai-Mongolia (Fig. 2) and Tuva-Mongolia units are an example of such a reactivated belt.

The Altai ranges (Fig. 1) generally strike NW-SE, while to the north they fan out in E-W ranges in their western part and N-S ranges in the east. Relief and elevation is most outspoken in the South Siberian Altai with peaks exceeding 4000 m (Belukha peak, 4506 m). In the north the Altai border is the West Siberian Basin: the Kuznetsk (east) and Biya-Barnaul (west) subbasins, in particular. To the SW the Altai are separated from the Zaisan-Junggar basin by the Irtysh shear zone. In Mongolia, the Altai ranges taper out into the E-W trending Gobi Altai. East of Altai are the Sayan Mountains and the Mongolian Great Lake depression.

Despite recent advances in our understanding of CADZ formation and basement evolution, geochronologic and thermochronologic data is sparse, especially in the Altai region. Therefore, an important rationale for this study is to contribute to the chronometry of regional tectonics, and to the Meso-Cenozoic history of

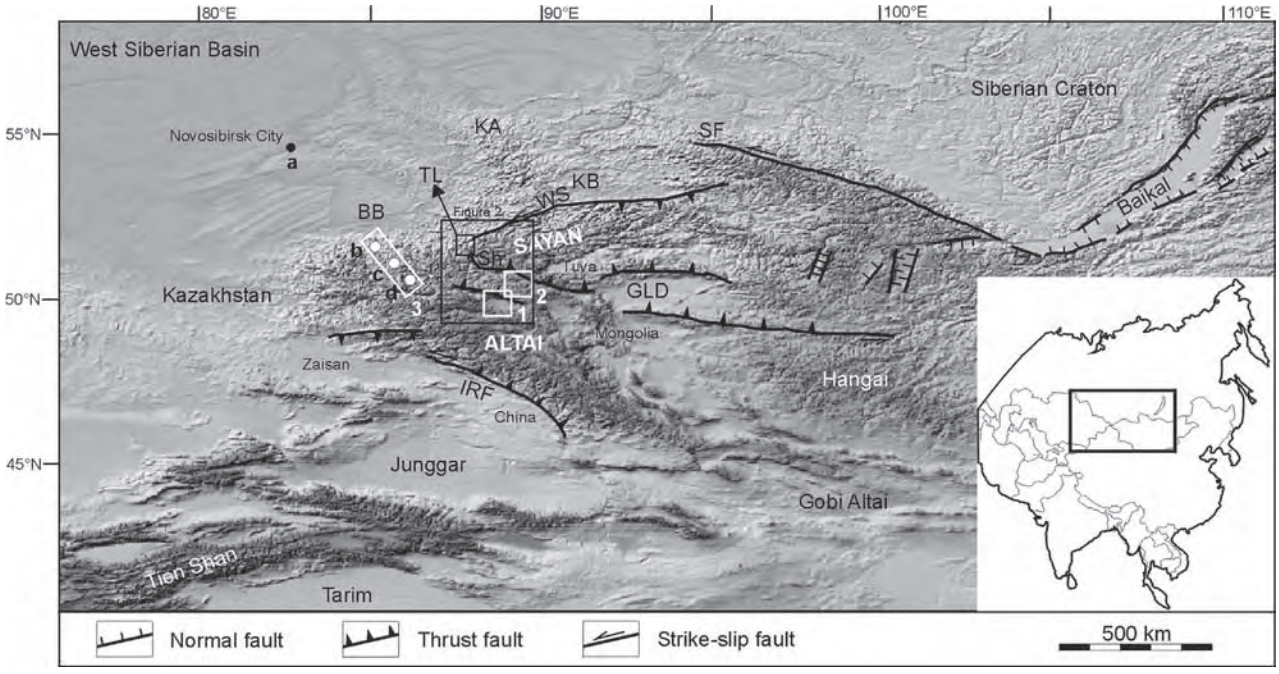

Fig. 1. Map of the Altai region in Central Asia. Sample locations are indicated by numbered boxes: (*1*) Chuya-Kurai Basin area, (*2*) Dzhulukul Basin area, and (*3*) western Gorny Altai transect (*a* = sample No-1; *b* = samples Be-1 and GA 01; *c* = GA 24; *d* = GA 03). *IRF* = Irtysh fault, *SF* = Sayan Fault, *Sh* = Shapshal Fault, *WS* = West Sayan fault. *BB* = Biya-Barnaul Basin, *GLD* = Great Lakes Depression in Mongolia, *KA* = Kuznetsk-Alatau Ridge, *KB* = Kuznetsk Basin.

the Siberian Altai. Because especially little is known about the Meso-Cenozoic history of the area, we opted to apply apatite fission-track (AFT) dating and modelling to basement rocks in order to try to find signals in low-temperature techniques that might help us constrain the chronology of the regional basement reactivation. Sediments in intramontane basins flanking our targeted basement-cored uplifts clearly record Meso-Cenozoic tectonic activity; however, from a basement perspective these events remain undisclosed.

2 Geological and Tectonic Setting

2.1 Paleozoic Geodynamics and Basement Structure

The Paleozoic of the Altai Mountains is dominated by the evolution of the Paleo-Asian Ocean (PAO) that extended south of Siberia (Buslov et al., 2001; Khain et al., 2003). During its final stage of evolution, several Paleozoic tectonic units, including terrains of the present-day Altai region, accreted to Siberia (Fig. 2), along an intricate network of sutures that was extensively reactivated with Late Paleozoic and Mesozoic strike-slip movements (Şengör et al., 1993; Buslov et al., 2003). Adding to the crustal growth of Siberia and Eurasia was the emplacement of huge amounts of syn- and post-collisional plutons (Dobretsov and Vladimirov, 2001; Fig. 2). In the Permian the PAO was consumed completely and subsequently, the Permo-Triassic was characterized by a period of tectonic quiescence, peneplanation, and red bed formation.

2.2 Meso-Cenozoic Reactivation and Formation of the Siberian Altai Orogen

From the Late Triassic and Jurassic on, sedimentary basins formed in a continental active tectonic regime (Dobretsov et al., 1995; 1996; Novikov, 2002). The Altai area was adjacent to several large basins where active subsidence and extension occurred. To the NW the West Siberian Basin, including the Kuznetsk and Biya-Barnaul sub-basins (Figs. 1, 3), was subjected to extension and rifting in the Jurassic-Cretaceous and terrigenous (molasse) and marine sediments were deposited (Pinous et al, 1999; Vyssotski et al., 2006). To the SW the Zaisan and Junggar Basin (Fig. 3) continuously subsided since the Permo-Triassic and accumulated km-scale thick Mesozoic sediments while its basement underwent reactivation in the Jurassic (Allen and Vincent, 1997). East of Altai several basins formed in the Great Lake Depression (GLD) of Mongolia and the Gobi (Fig. 3) where Mesozoic extension is widely documented and Jurassic-Cretaceous terri-

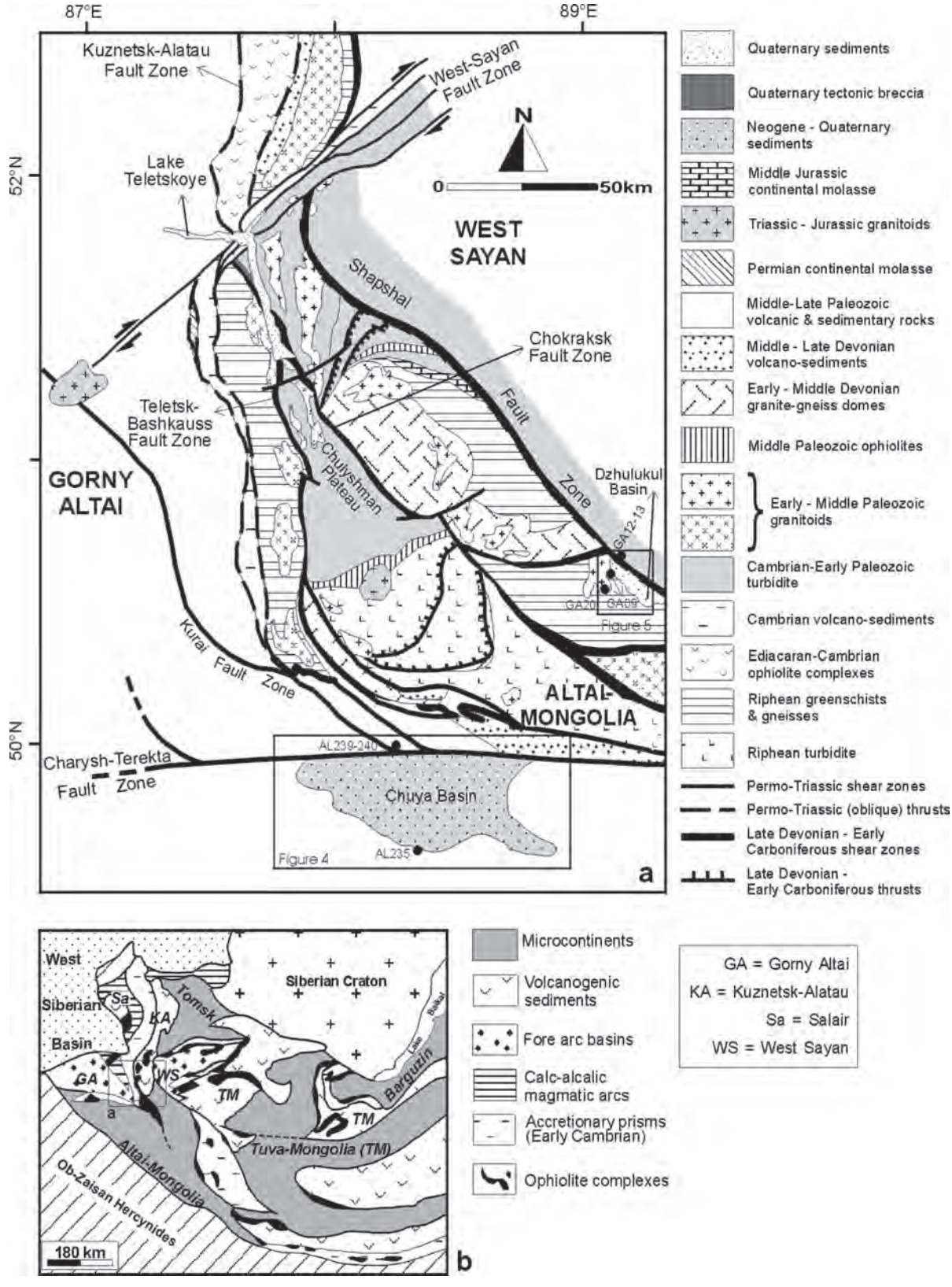

Fig. 2. **a** Simplified geological map of the Siberian Altai Mountains, **b** Schematic map of Paleozoic basement blocks in the Siberian Altai region.

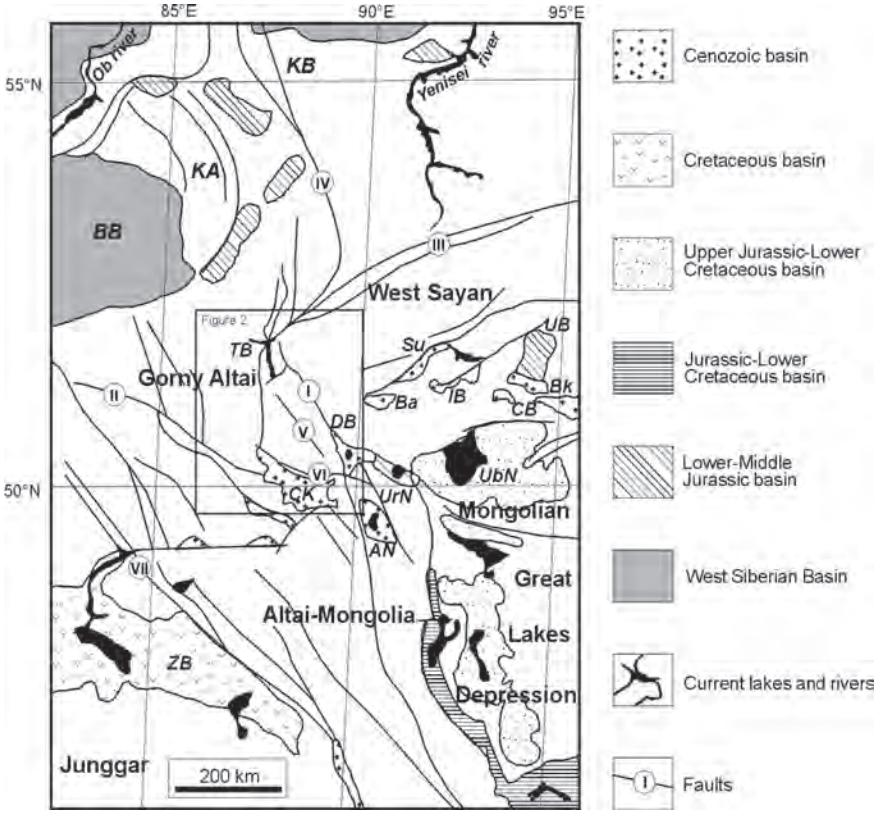

Fig. 3. Meso-Cenozoic basins in the Altai region (after Dobretsov et al., 1996). Basins: *AN* = Achit Nuur, *Ba* = Barlik, *BB* = Biya-Barnaul, *Bk* = Baikhak, *CB* = Chagyshai Basin, *CK* = Chuya-Kurai, *DB* = Dzhulukul Basin, *IB* = Initial Basin, *KA* = Kuznetsk-Alatau thrust, *KB* = Kuznetsk Basin, *Su* = Sutkol, *TB* = Teletskoye Basin, *UB* = Uluchkhem Basin, *UbN* = Ubsu-Nuur, *UrN* = Ureg-Nuur, *ZB* = Zaisan Basin. Faults: *I* = Shapshal; *II* = Charysh-Terekta, *III* = West Sayan, *IV* = Kuznetsk-Alatau, *V* = Chulyshman, *VI* = Kurai, *VII* = Irtysh.

geneous sediments accumulated (Graham et al., 2001; Johnson, 2004). North and east of the GLD, the Mongol-Okhotsk Ocean between Siberia and North China–Mongolia (Amuria) closed. Collision of these continents induced the Mongol-Okhotsk orogeny that affected a broad region in Mongolia, North China, and Siberia (Delvaux et al., 1995a; Zorin, 1999; Kravchinsky et al., 2002; Tomurtogoo et al., 2005). The collision was diachronous: the suture is younger from west (Permo-Triassic) to east (Early Cretaceous).

Tectonic forces from the adjacent Mesozoic active provinces affected the Altai basement in the Late Jurassic-Cretaceous. In the Siberian Altai Jurassic fault-controlled basins developed along the Shapshal fault zone and accumulated continental molasse and other coarse Jurassic sediments (Dobretsov et al., 1996; Novikov, 2002; Fig. 2). This implies a Jurassic denudation-sedimentation event in the Siberian Altai, coeval with sedimentation in the larger adjacent basins mentioned. Tectonic activity was accompanied by emplacement of Triassic-Jurassic plutons (Dobretsov and Vladimirov, 2001). In the Cretaceous-Paleogene, tectonic activity subsided and the area experienced peneplanation (Delvaux et al., 1995a and 1995b; Nikolaeva and Shuvalov, 1995; Dehandschutter et al., 2002). Similar Mesozoic tectonic signatures were observed for the Mongolian Altai (Howard et al., 2003).

After Early Cenozoic quiescence, Late Cenozoic and active tectonism related to ongoing indentation of India into Eurasia developed a series of active intracontinental mountain belts through Central Asia. The distant tectonic effects of India-Eurasia convergence have reactivated some of the major Paleozoic structures within the Siberian Altai basement and are responsible for the Late Cenozoic building and morphology of the modern Altai orogen.

The Cenozoic history of the Siberian Altai can be described based on the evolution of the Chuya basin (Fig. 4). A complete ~1.5-km-thick Late Cretaceous to recent stratigraphic section is preserved (Delvaux et al., 1995b; Zykin and Kazansky, 1995; Buslov et al., 1999). The basin is situated in the Gorny Altai tectonic unit (Fig. 2) and its basement is composed of Ediacaran-Cambrian volcanic arc and accretionary prism rocks and Devonian active margin deposits (Buslov and Watanabe, 1996). Remnants of the Cretaceous–Paleogene peneplain are preserved on top of some basement blocks adjacent to the basin (Novikov et al., 1998). Late Cretaceous sediments found in small, remnant basins in the Charysh-Terekta strike-slip fault zone, just west of the Chuya basin (Fig. 4), contain marine radiolaria and foraminifers and represent a transgression from a Cretaceous seaway to the West Siberian Basin (Zykin et al., 1999). Currently these marine sediments are at

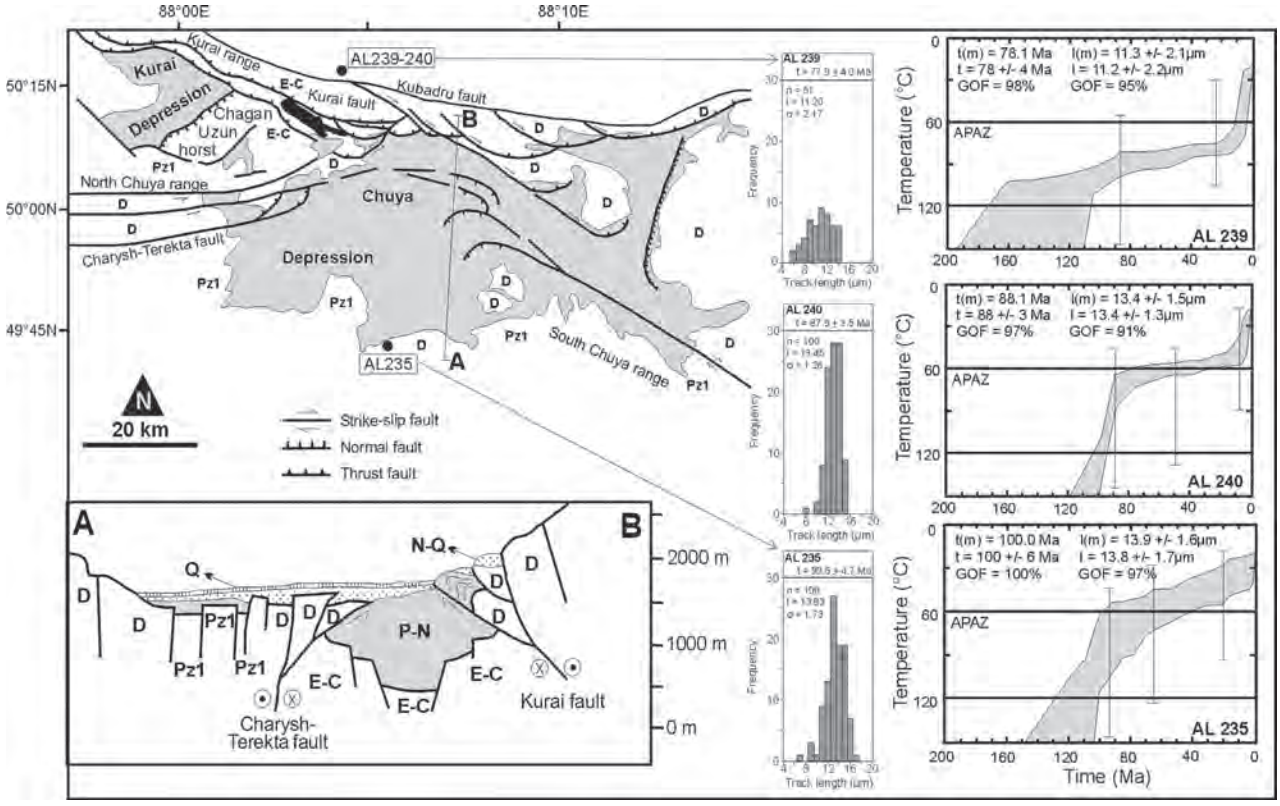

Fig. 4. Structural and geological sketch map and cross-section (AB) of the Chuya-Kurai Basin and Ranges (southern Siberian Altai). Sample locations are indicated by black dots. AFT age and length data are shown: *t* = AFT age, *n* = number of measured confined tracks, *l* = mean track length, *σ* = standard deviation of track length distribution. Thermal history models for these samples are also indicated. Modelling was performed using Laslett et al. (1987) annealing equations and the AFTSolve software by Ketcham et al. (2000). *APAZ* = Apatite Partial Annealing Zone; *t* (*m*) = modeled AFT age, *t* = observed AFT age, *l* (*m*) = modeled mean track length, *l* = observed mean track length; *GOF* = Goodness of fit. The best statistical tT-path is represented by a line within a statistical good fits envelope (shaded). See text for description and interpretation. For sample details see table 1. *Pz1* = undivided Lower Paleozoic units, *E-C* = Ediacaran-Cambrian island arc rocks, *D* = Devonian active margin units, *N-Q* = Neogene-Quaternary sediments, *Q* = Quaternary sediments.

an elevation of over 1500 m. Reworked material from these sediments and the Late Cretaceous–Paleogene peneplain are found in the basal Karachum Formation of the Chuya Basin. In these incipient stages, the basin developed as a strike-slip basin (Delvaux et al., 1995b). The basal section is dated to the Late Paleocene–Eocene (perhaps Early Oligocene) based on plant and pollen fossils (Zykin and Kazansky, 1995; Buslov et al., 1999). Oligocene lacustrine sediments are fine (clays, marls, fine sands) and contain pollen fossils that point towards a shallow, low-elevation lake basin, representing an embryonic stage of renewed tectonism. Similar observations were made in the adjacent Mongolian Altai area (Howard et al., 2003). This situation persisted in the Miocene and is encountered in other Siberian Altai locations (e.g. Dzhulukul Basin) (Dobretsov et al., 1996; Novikov, 2002). Towards the Late Miocene–Early Pliocene coarse sands appear and by the Late Pliocene (~3 Ma ago; Buslov et al., 1999), coarse sands, breccias, and conglomerates dominate and demonstrate basin inversion and growth of the bordering Chuya and Kurai ranges that today house some of the highest Altai peaks (>4000 m). The Late Pliocene is therefore thought to be the time of onset of regional reactivation of the Gorny Altai unit. This reactivation is mainly transpressive with counterclockwise rotation (Thomas et al., 2002) and significant strike-slip. Thrust or reverse faulting positioned hanging wall Paleozoic basement blocks on Plio-Pleistocene glacial sediments during the Late Pleistocene-Quaternary as the Chuya basin evolved to a half- and full-ramp basin (Delvaux et al., 1995b; Buslov et al., 1999). The neotectonic evolution is dominated by reactivation of Paleozoic faults (Kurai and Charysh-Terekta; Fig. 4). A recent (27 Sept. 2003) strong (M = 7.3) earthquake induced by strike-slip along Charysh-Terekta shows its continued activity. Building of the Siberian Altai mountain ranges largely occurred since the

Late Pliocene. This young tectonic activity is mainly manifested along reactivated Paleozoic structures (e.g. Dehandschutter et al., 2002).

Similar Late Cenozoic and active transpressive intracontinental tectonics and orogenic development of the Mongolian and Chinese Altai have been documented by structural (Cunningham et al., 1996), (paleo)seismic (Pollitz et al., 2003; Vergnolle et al., 2003), geomorphologic, remote sensing (Philip and Ritz, 1999) and geodetic methods (Calais et al., 2003). However, in contrast to the Siberian Altai, earlier signs of coarse-clastic erosion and uplift (Miocene and Late Oligocene) are recorded, while the Pliocene is also characterized by the deposition of molasse-type sediments in intramontane basins (Howard et al., 2003). This implies that since the Pliocene an orogen-wide tectonic pulse affected and shaped the Altai as a whole, while earlier (Miocene) signs are recorded in the Mongolian Altai.

3 Samples, Sample Areas, and Analytical Procedures

Sample localities in the Siberian Altai Mountains are grouped in three distinct areas:

1. The Chuya-Kurai Basin and Ranges,
2. The Shapshal Range and Dzhulukul Basin
3. The western Altai transect (Gorny Altai).

All samples (Table. 1) are from Paleozoic basement involved in Late Cenozoic reactivation and characterized by nearby deposition of related Late Cenozoic clastic sediments. The sample sites, especially the Chuya-Kurai and Dzhulukul Basins, are typified by reverse or thrust faults connected to adjacent intramontane basins.

3.1 The Chuya-Kurai Basin and the Chuya and Kurai Ranges

The Chuya-Kurai Basin is located at the junction zone of the Gorny Altai, West Sayan, and Altai-Mongolia tectonic units (Fig. 2). Once a continuous Cenozoic depression, the Chuya and Kurai basins are presently separated by the Chagan-Uzun horst (Fig. 4). Their sediments span the entire Cenozoic as discussed in detail earlier. Cenozoic movements of the Paleozoic rocks from the bordering Kurai and Chuya ranges have deformed the sediments. Fault movements were lateral (strike-slip) with a clear vertical component of either reverse faulting (steep fault plane) or thrusting (low angle fault). The basin is hence bordered by positive, left lateral flower systems, giving the basin a ramp-like morphology (Delvaux et al., 1995b; Buslov et al., 1999). We analyzed two samples (AL 239-240, Table. 1, Fig. 4) from the Kurai Range and a granodiorite sample from the South Chuya Range (AL 235).

Table 1. Location and description of AFT samples from the Siberian Altai Mountains

Sample	Latitude	Longitude	Altitude	Locality	Lithology
1. Chuya-Kurai Basin					
AL 235	49°44′06″N	88°05′50″E	3490 m	Dzankiol pass	pegmatite
AL 239	50°16′31″N	88°04′25″E	2720 m	Ildugemsky pass	mylonite
AL 240	50°16′00″N	88°04′00″E	2440 m	Ildugemsky pass	granodiorite
2. Dzhulukul Basin					
GA 09	50°43′00″N	89°15′17″E	2240 m	Mayrikbazhi massif	gneiss
GA 12	50°45′50″N	89°18′10″E	2785 m	Trechglavaya massif	granodiorite
GA 13	50°45′11″N	89°19′28″E	2500 m	Trechglavaya massif	granodiorite
GA 20	50°37′54″N	89°14′18″E	2015 m	Uzun Uyok river	granitic aplite
3. Western Gorny Altai					
Be 1	51°56′24″N	84°45′24″E	290 m	Belokuriha massif	granite
GA 01	51°55′16″N	85°51′15″E	295 m	Rybalka massif (Sausga)	granodiorite
GA 03	50°38′59″N	86°17′54″E	1100 m	Chiquetaman pass	granodiorite
GA 24	51°19′48″N	85°40′14″E	840 m	Shebalino village	rhyolite
4. Novosibirsk					
No 1	54°59′15″N	82°59′12″E	90 m	Borok quarry, Priobsky complex	monzodiorite

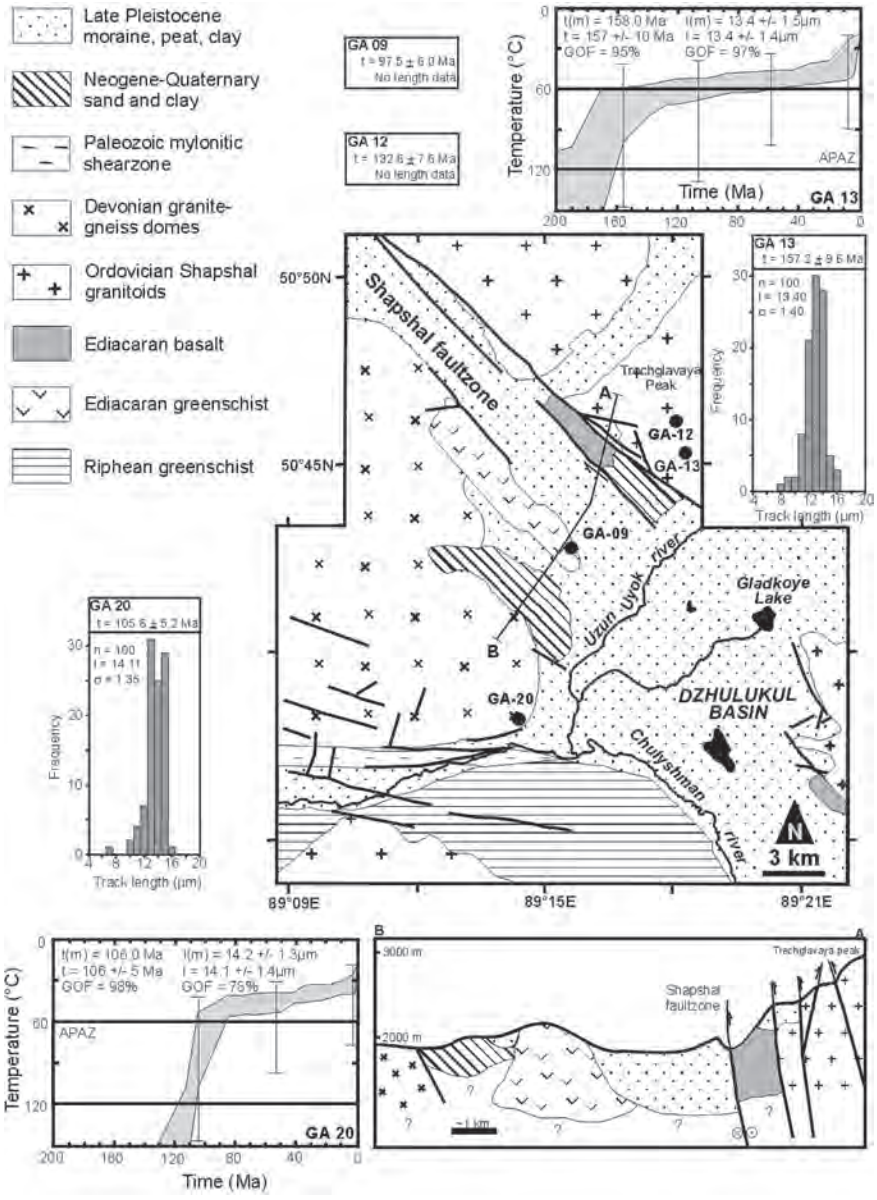

Fig. 5. Structural and geological sketch map and cross-section (AB) of the Dzhulukul Basin (eastern Siberian Altai). Sample locations are indicated by black dots. AFT age and length data are shown: abbreviations and symbols are identical as in Fig. 4. See text for description and interpretation. For sample details see Table 1.

3.2 The Dzhulukul Basin and the Shapshal Range

The Cenozoic Dzhulukul Basin developed along the transpressive reactivated Shapshal fault as a full ramp basin (Figs. 2, 5). Its basement consists of Late Precambrian-Early Paleozoic greenschist and gneiss. At present the Dzhulukul basin resides at an elevation of ~2000 m. Its morphology and sediments are clearly influenced by glacial activity and erosion. The basin is mainly filled with Cenozoic glacial deposits and moraines, intercalated with peat horizons. Novikov (2002) observed that the basin contains small pockets of Jurassic basal units on which the Cenozoic sediments rest unconformably as is the case in many adjacent basins in western Mongolia. To the east the basin is flanked by the Ordovician granitoids of the Shapshal range with Ediacaran basalts at its base. The range is obliquely thrust on Dzhulukul sediments along the Shapshal fault as a result of Late Cenozoic transpressive reactivation. Active tectonic movements along the fault and related structures in Mongolia have resulted in strong historic earthquakes and foreberg formation (Bayasgalan et al., 1999). One Dzhulukul basement gneiss (GA 20) and three Shapshal granitoid samples (GA 09, GA 12, and GA 13) (Table.1, Fig. 5) were obtained.

3.3 The Western Gorny Altai Transect

Also samples in Gorny Altai were collected (general location: Fig. 1) along the main road from the city of Gornyaltaisk to Tashanta at the Mongolian border. This road transects the western Chulyshman and Kurai areas and the lower, hilly foreland areas of NW Gorny Altai. Samples from this area, the 'Western Gorny Altai Transect' come from several Paleozoic plutons and igneous complexes: (1) the Permo-Triassic Belokurikhinsky lacolith (sample Be-1) at the junction between the reactivated modern orogen and the stable Biya-Barnaul Basin, (2) the Devonian Rybalka granitoid-gabbroid massif (GA-01), (3) the Late Devonian Chiquetaman granitoid massif (GA-03), and (4) the Devonian Shebalino rhyolite (GA-24) (active margin sequence). An additional sample (No-1, monzodiorite) was collected near Novosibirsk city (Borok quarry, Permo-Triassic Priobsky batholith), in the eastern part of the flat and stable platform of the West Siberian Basin. No Cenozoic tectonic reactivation is seen here.

3.4. Analytical Procedures

The apatite from aforementioned samples was separated using conventional heavy liquid and magnetic techniques, embedded in epoxy, polished, and dated with the external detector (ED) method. Muscovite mica (Goodfellow clear ruby) was used as an ED. Spontaneous tracks in the apatite were etched with a 2.5% HNO_3 solution for 70 s at 22°C. Induced tracks in the ED were etched with a 40% HF solution for 40 minutes at 22°C. Apatite-ED wafers were irradiated in several batches in the well-thermalized channels of the Thetis research reactor facility at the University of Gent. Depending on the irradiation, thermal neutron fluence values of around 2×10^{15} cm^{-2} were achieved. The thermal neutron fluence was monitored using metal activation monitors, i.e., diluted Au-Al and Co-Al alloys (e.g., Van den haute et al., 1998).

Track counting and length measurements were done using an Olympus BH-2 optical microscope with a 1250× magnification (10× eyepieces with counting grid, 100× dry objective, 1.25× drawing tube attachment) equipped with transmitted and reflected light. At least 1000 spontaneous tracks were counted per sample, spread over minimum 20 separate grains; where possible 100 confined tracks were measured to construct an AFT length-frequency distribution and a mean track length (MTL) was calculated. AFT age and length data were modeled using the Laslett et al. (1987) annealing equations and the AFTSolve modelling software by Ketcham et al. (2000).

The apatites were dated using both an absolute approach based on the procedure factor (Q) and using a fission decay constant (λ_f) of 8.46×10^{-17} a^{-1} (e.g. Wagner, and Van den haute, 1992; Jonckheere, 2003) and the conventional zeta (ζ) method (Hurford and Green, 1983; Hurford, 1990). An overall weighted mean zeta (OWMZ) was calculated on the basis of 32 apatite age standard mounts of Durango and Fish Canyon Tuff apatite (Hurford and Green, 1983). The IRMM-540 dosimeter glass (De Corte et al., 1998) was used and our OWMZ calibration factor was determined as 253.1 ± 2.4. Only conventional mean ζ-ages were used for the thermal history modelling. In all our irradiation packages, apatite age standards co-embedded with dosimeter glass shards, as well as foils of diluted Co-Al and Au-Al metal activation monitors, were included. These were spaced with regular intervals throughout the sample package in order to detect and correct for a possible axial thermal neutron fluence gradient. It also allowed for the interpolation of fluence values (absolute calibration) and induced glass dosimeter track densities (ρ_d for ζ calibration) for each sample individually.

4. AFT Results and Thermal History Modelling

AFT age and length data (Table. 2) is indicated on the sample area maps: Chuya-Kurai basin (Fig. 4), Dzhulukul basin and Shapshal Range (Fig. 5), and the western Gorny Altai transect and Novosibirsk sample (Fig. 6). AFT ages are conventional ζ-ages (Hurford, 1990). Track lengths were measured on natural horizontal confined tracks. Not all samples yielded sufficient confined tracks and hence no length data is reported for those samples. AFT age and length data were modelled using the Laslett et al. (1987) annealing model (with initial track length parameter l_o = 16.3 μm) and the AFTSolve thermal history modelling software (Ketcham et al., 2000). Thermal history models and length distributions are shown (Figs. 4, 5, 6). Statistical good fits (Ketcham et al. 2000) are shown as a shaded tT-envelope. Interpretation and discussion is based on the general model trends (good fits envelope). In a first run a model was only constrained by two tT constraints: a low-T (~10°C) benchmark reflecting current ambient temperatures, and a high-T bar-constraint well above 120°C (AFT accumulation threshold) far enough back in time, i.e., significantly predating apparent AFT ages. An age of ~260 Ma was chosen based on Permian amphibole $^{40}Ar/^{39}Ar$ ages (regional Permian strike-slip deformation) from the Teletskoye area in the northern Siberian Altai (Dehandschutter et al., 1997). After an initial run, additional constraints were placed reiteratively along the general thermal history trend to refine the model. Care was taken to place as

Table 2. AFT age and length data for the Siberian Altai samples. ρ_s, ρ_i, and ρ_d are respectively, the density of spontaneous, induced tracks and induced tracks in an ED irradiated against a dosimeter glass. The ρ_d-values are interpolated values obtained from regularly spaced glass dosimeters in each of the irradiation packages, expressed as 10^5 tracks/cm^2. Values for ρ_s and ρ_i are expressed as 10^6 tracks/cm^2. N_s, N_i, and N_d are respectively, the number of counted spontaneous, induced tracks and induced tracks in an ED irradiated against a dosimeter glass. N_d is also an interpolated value. $P(\chi^2)$ is the chi-squared probability that the dated grains have a constant ρ_s/ρ_i-ratio, it is given on a 0 to 1 scale. An OWMZ value of 253.1±2.4 a·cm^2 (Durango and Fish Canyon Tuff apatite age standards and the IRMM-540 dosimeter glass) was used for the calculation of t(ζ). AFT length data are reported as a mean track length (l_m) with standard deviation, σ, obtained from the measurement of a number (n) of natural, horizontal confined tracks.

Sample	Grains	ρ_s (± 1σ)	N_s	ρ_i (± 1σ)	N_i	ρ_d (± 1σ)	N_d	$P(\chi^2)$	t(ζ) in Ma	l_m (µm)	n	σ (µm)
1. Chuya-Kurai Basin												
AL 235	30	2.175 (0.055)	1580	1.263 (0.042)	912	4.113 (0.080)	2633	0.36	99.6 ± 4.7	13.8	100	1.7
AL 239	50	1.219 (0.032)	1486	0.683 (0.024)	832	3.315 (0.083)	1614	1.00	77.9 ± 4.0	11.2	51	2.2
AL 240	30	1.657 (0.026)	3937	0.950 (0.020)	2257	3.934 (0.111)	1259	1.00	87.9 ± 3.5	13.5	100	1.3
2. Dzhulukul Basin												
GA 09	30	2.009 (0.068)	862	0.992 (0.046)	457	4.054 (0.080)	2595	0.99	97.5 ± 6.0	---	---	---
GA 12	30	3.433 (0.100)	1188	1.407 (0.063)	503	4.049 (0.079)	2592	0.30	132.6 ± 7.6	---	---	---
GA 13	30	2.846 (0.078)	1332	0.872 (0.043)	408	3.851 (0.083)	2169	0.99	157.2 ± 9.6	13.4	100	1.4
GA 20	20	1.197 (0.031)	1532	0.588 (0.021)	753	4.024 (0.079)	2576	0.76	105.6 ± 5.2	14.1	100	1.4
3. Western Gorny Altai and Novosibirsk												
Be 1	30	0.951 (0.030)	979	0.525 (0.022)	551	4.108 (0.080)	2629	0.99	99.1 ± 5.7	13.7	32	1.6
No 1	50	4.246 (0.082)	2682	1.296 (0.046)	788	4.078 (0.080)	2610	0.54	178.6 ± 8.2	---	---	---
GA 01	50	1.739 (0.051)	1144	0.777 (0.034)	510	4.073 (0.080)	2607	1.00	120.4 ± 6.9	13.3	60	2.0
GA 03	40	0.899 0.032)	809	0.447 (0.022)	402	3.858 (0.083)	2173	1.00	98.8 ± 6.5	13.6	58	1.9
GA 24	17	3.551 (0.110)	1044	1.131 (0.062)	338	4.014 (0.079)	2569	0.81	165.5 ± 11.0	---	---	---

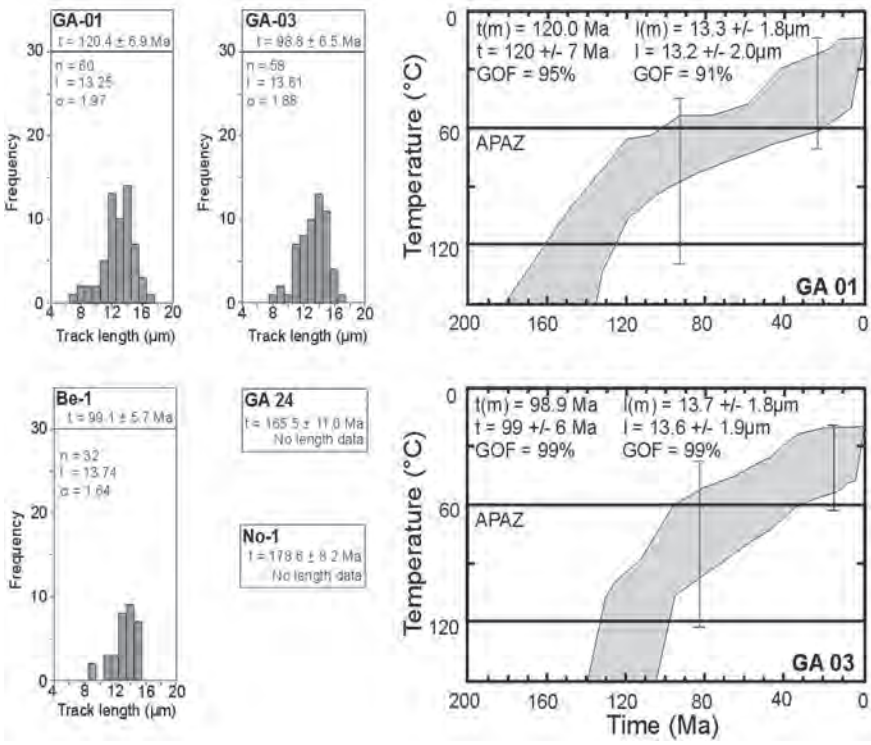

Fig. 6. AFT age and length data from the Western Gorny Altai Transect samples: AFT age and length data are shown: abbreviations and symbols are identical as in Fig. 4. See text for description and interpretation. For sample details see Table 1 and Fig. 1

few constraints as possible, and to let the T-interval be as wide as possible (i.e., wider than the statistically acceptable tT-paths envelope; Ketcham et al., 2000).

No reset Cenozoic AFT ages were found. Apparent AFT ages are Late Jurassic-Cretaceous and range between 80 and 160 Ma, except the Early Jurassic age (179 Ma) for the Novosibirsk sample (No-1, Table. 2). In particular, we obtained the following ages: (1) Chuya-Kurai area: 80–100 Ma (elevations ~2500–3500 m), (2) Dzhulukul: 100–160 Ma (elevations ~2000–2800 m), and (3) western transect: 100–165 Ma (elevations ~300–1000 m). No clear regional trend can be detected, except that lower ages are found in the high elevation area of Chuya-Kurai, higher ages in the lower foreland and intermediate ages in the Dzhulukul area. In general, higher elevation samples from a single area yield higher ages. Mean track lengths (MTL) and length distributions show clear signs of thermal track shortening, suggesting a prolonged stay at APAZ temperatures (120–60°C) (Wagner and Van den haute, 1992). MTL values vary between 11–14 μm (with most around 13 μm), distributions are generally broad ($1.3 < \sigma < 2.2$ μm), asymmetric, and negatively skewed (Figs. 4, 5, 6).

The AFT age and length data was modelled according to the principles mentioned earlier and a two- and possibly three-stage thermal history model was reconstructed: (1) Cretaceous rapid cooling, (2) Late Cretaceous-Paleogene stability with only slow cooling, and a possible (3) Late Neogene-Quaternary cooling (Figs. 4, 5, 6). The latter event is only clearly registered in sample AL239, while it is only suggested (outside the 120–60°C T-interval) in the other samples. However, the models calculated here are in good agreement with these from samples in the northern Siberian Altai where the younger stage (3) is more outspoken (De Grave and Van den haute, 2002) and the Chinese Altai (Yuan et al., 2006). Sample GA-13, collected east of the Shapshal fault (Fig. 5) shows an earlier onset of Mesozoic cooling, while all other samples show a later onset. These all originate from areas west of the Shapshal fault. This might suggest that cooling of the Altai basement was diachronous, possible related to differential block movements along the Shapshal fault zone in a Mesozoic phase of reactivation.

The Cretaceous event cooled the investigated apatites below the 120°C threshold roughly ~120 Ma ago. Considering a normal geothermal gradient of 25–30 °C/km, this implies that most of our apatite bearing rock samples were brought to depths shallower than ~4 km in the crust. According to the general trend in our thermal history models, the Cretaceous cooling lasted until ~80–90 Ma ago. At the cessation of this cooling, the sampled rocks were at upper APAZ to lower AFT retention temperatures (~80–50°C), corresponding to a depth of 3–2 km considering a geothermal gradient of 25–30 °C/km. At these conditions partial AFT annealing persisted and tracks shortened. Variations of these modelled values is predominantly due to their present outcrop altitude, and hence their associated paleo-depth. Additional scatter (e.g., between samples AL239 and 240) might be due to chemical composition differences between individual apatites (Green et al., 1986).

After Cretaceous cooling near-horizontal tT-paths endured from the Late Cretaceous, throughout the Paleogene, until the Late Miocene. This stage in the general thermal history marks a period of stability or slow cooling during which the sampled rocks stayed at upper APAZ/lower retention temperatures. The near-horizontal tT-paths are disturbed by rapid Pliocene to Recent cooling, starting about 15–5 Ma ago. This is evident from sample AL 239, while this event in our models for the other samples falls below the 60°C isotherm. This young rapid cooling eventually brought the samples to ambient surface temperatures and is associated with the exhumation of the apatite bearing rocks to their present outcrop positions. The long APAZ residence time (Late Mesozoic to Late Cenozoic) and associated track annealing and shortening explains the low MTL values and broad, negatively skewed track length distributions (Figs. 4, 5, 6).

A note of caution concerning the Late Cenozoic cooling event should be conveyed here. It has been shown that there exists a potential in AFT thermal history models using specific model parameter values (lo parameter) to produce Late Cenozoic cooling merely as an artefact. This artefact, the 'worldwide recent cooling' (Ketcham et al., 1999; 2000) can further be enhanced by track annealing at ambient temperatures. It is therefore hazardous to interpret Late Cenozoic cooling merely based on AFT thermal history models. It should be meticulously tested against independent geological evidence, as we have attempted to do in this work.

5 Discussion, Tectonic Implications and Conclusions

5.1 The Cretaceous Cooling Event

Cretaceous cooling of the Siberian Altai basement is contemporaneous with an important denudation event in the Jurassic-Cretaceous as recorded in the sediments of intramontane Altai basins and larger orogen-adjacent basins (Figs. 2, 3). We therefore interpret the Mesozoic AFT ages (Table. 2) and the Cretaceous cooling observed in the thermal history models as Siberian Altai basement denudation. Considering a geothermal gradient of 25–30°C/km, the Siberian Al-

tai experienced at least 1 to 3 km of Late Jurassic-Cretaceous denudation recorded by the AFT system.

The derived sediments were mainly fluvially transported to large adjacent basins (GLD, West Siberian Basin, Junggar-Zaisan Basin), and to smaller fault-controlled, intramontane depressions (Dobretsov et al., 1996; Pinous et al., 1999; Howard et al., 2003; Vyssotski et al., 2006). Mesozoic sediments, mainly Jurassic and Early Cretaceous deposits, unconformably overlie the Paleozoic basement of these basins. Mesozoic sediment thickness reaches several kilometers in the large adjacent basins, and in the smaller intramontane basins it locally reaches over 2 km. In these intramontane basins, Mesozoic sediments are often molassic type deposits. The facts that the Altai basement is subjected to significant cooling as seen in the AFT data, that derived sediments are coarse-grained and deposited in thick sequences in large adjacent basins and in fault-controlled basins in the Altai orogen itself, point to denudation of a reactivated orogen. This hypothesis is further underscored by the occurrence of the Late Mesozoic Kuznetsk-Alatau thrust system and related basins at the northern edge (Salair Ridge) of the present-day Altai orogen (Fig. 3), at the Kuznetsk Basin interface (Novikov, 2002; Buslov et al., 2003). The kinematics, and tectonic-geodynamic implications of this thrust system are poorly understood and form the subject of ongoing research. It however clearly indicates Jurassic-Cretaceous tectonic activity in the Siberian Altai.

Accommodation of thick Mesozoic deposits and evidence from geophysical exploration in the large adjacent basins also indicates active extension, and subsidence within these basins: the West Siberian Basin (Pinous et al., 1999; Vyssotski et al., 2006), the Mongolian-Baikal and Junggar basins (Graham et al., 2001; Johnson, 2004). Therefore, denudation and subsequent cooling of the basement as observed in our models, was most likely a complex interaction of extension in large adjoining basins creating accommodation space for Altai deposits on one hand, and tectonic reactivation of the Altai orogen on the other.

Mesozoic tectonic reactivation of the Altai Mountains is coeval with the final stages of closure of the Mongol-Okhotsk (MO) Ocean, and the ensuing MO orogeny. Convergence and ultimate collision of the Siberian and North Chinese-Mongolian continent or Amurian plate, resulted in the development of the MO orogenic belt in the Late Jurassic-Early Cretaceous (Zorin, 1999; Kravchinsky et al., 2002; Tomurtogoo et al., 2005). Incipient collision occurred in the western part of the MO belt (South Baikal - East Sayan - Mongolia area) around the Lias-Dogger transition (170–180 Ma ago). Oblique collision and associated diachronous compressive tectonics lasted until final closure of the MO Ocean in the east during the Early Cretaceous (110–140 Ma ago). Deformation was not solely confined to the collision zone proper, but migrated through the hinterland and affected the Mongolian Altai (Dobretsov et al., 1996), the Baikal area (Van der Beek et al., 1996) and reached the Siberian cratonic rim (Zorin, 1999). Our AFT data imply that the Siberian Altai region also experienced far-field effects of the MO orogeny. This induced reactivation and deformation of the ancestral Altai, and to an important phase of denudation as discerned from the Mesozoic tT-cooling paths in our thermal history models. Van der Beek et al. (1996) interpret AFT results of Mesozoic denudation in the Baikal area also in terms of distant effects of the MO orogeny. Their AFT ages and thermal history models show a Late Cretaceous cooling, which is somewhat younger than our results. This is in agreement however with the oblique collision model as outlined above, where initial collision and orogeny affected the western area (Altai) earlier with respect to the central (Baikal) and eastern parts of the MO belt. A similar pattern in pluton emplacement ages along the collision zone corroborates this model (Tomurtogoo et al., 2005). Yuan et al. (2006) however interpret Cretaceous apparent AFT ages and a Cretaceous cooling obtained from thermal history models from the Chinese Altai as a possible consequence of the collision of Eurasia with the Lhasa block (Tibet) and the related Cimmerian orogeny. However, Cimmerian effects in Central Asia are generally older and of Late Jurassic-Early Cretaceous age (e.g. Sobel and Dumitru, 1997; Bullen et al., 2001; De Grave et al., accepted).

5.2 The Period of Late Cretaceous-Paleogene stability

Near horizontal tT-paths at lower APAZ to upper AFT retention temperatures (50–80°C) in the Late Cretaceous-Paleogene reflect a period of prolonged stability in the Siberian Altai. While some samples clearly show a horizontal tT trend (e.g. AL239 or 240), others exhibit a continuous slow cooling (e.g. GA 03). During this period intracontinental Siberia and Central Asia experienced tectonic quiescence and the Mesozoic orogen was subjected to peneplanation. Rocks consequently remained approximately at the position and depth in the crust they reached after the Mesozoic denudation phase. This implies that relaxation of the isotherms occurred and that these rocks stayed at more or less constant temperatures as reflected by the near-horizontal tT-paths in our thermal history models. In Siberia and Central Asia a vast lateritic peneplain with typical red beds developed (Delvaux et al., 1995a and 1995b; Nikolaeva and Shuvalov, 1995; Dobretsov et al., 1996). Remnants of this peneplain are found in many parts of the region, and also in the Siberian Altai

(Novikov, 2002; Dehandschutter et al., 2002). At present the surface is extensively deformed as a result of Late Cenozoic tectonic activity. Remnants are mainly found on plateau-like uplifts, or as basal sequences in Cenozoic intramontane basins (Chuya-Kurai Basin), and are vertically offset by hundreds of meters. This interpretation agrees with observations and interpretations of AFT cooling curves for the adjoining Baikal region (Van der Beek et al., 1996).

5.3. The Late Cenozoic Cooling Event

The Late Cenozoic cooling phase in our thermal history models for the Chuya-Kurai area is associated with the tectonic reactivation of the region and the building and denudation of the modern Altai. The reactivation is thought to be a far-field effect of the India-Eurasia collision and the ongoing indentation of the Indian plate into the Eurasian continent. According to the AL239 model, cooling commenced between 15-5 Ma ago and continues until the present. This corresponds with other indicators that point towards initiation of reactivation in the Late Neogene and clear intensification of transpressive tectonic movements in the Plio-Pleistocene (Cunningham et al., 1996; Dobretsov et al., 1996; Buslov et al., 1999; Dehandschutter, 2002; Novikov, 2002; Howard et al., 2003). This event is more outspoken in earlier AFT studies in the northern part of the Siberian Altai, e.g., in the Teletskoye area (Fig. 1) (De Grave and Van den haute, 2002). Sediments produced by the denudation of the modern Altai orogen are deposited in the large adjacent basins (West Siberian Basin, Mongolian GLD, Junggar-Zaisan Basin) in a similar setting as during the Mesozoic denudation (Fig. 3). Also reminiscent of the Mesozoic denudation, formation of Cenozoic, fault-controlled intramontane basins accommodate part of the Late Cenozoic sediments derived from the growing orogen. The Dzhulukul and Chuya-Kurai Basins are important examples. In these basins, several horizons of coarse Late Neogene to Quaternary sediments are observed (Delvaux et al., 1995b; Buslov et al., 1999; Dehandschutter et al., 2002).

Late Cenozoic reactivation of the Siberian Altai Mountains is substantiated by deformation of the Late Cretaceous-Paleogene peneplain. In comparison to the low-lying inactive hinterland, peneplain remnants are vertically displaced by 2 km or more (Dehandschutter et al., 2002), while in mountain ranges and plateau-like uplifts, adjacent blocks capped with remnants of the lateritic peneplain show vertical offsets of hundreds of meters relative to each other. Preservation of the peneplanation surface however puts an upper limit on the extent of post-Paleogene denudation and on the magnitude of concomitant cooling observed in our AL239 thermal history model. Preservation is local, not regional, indicating that some of the blocks were indeed subjected to considerable denudation. In addition, all samples were collected at the surface and along vertical profiles situated well below the estimated position of the peneplain. In summary, while tectonic and sedimentary evidence indicates a Late Neogene-Quaternary episode of intense tectonic activity with rapid uplift and sedimentation in the Siberian Altai, the AFT models only record the event clearly for sample AL239 in the Chuya region, while other samples suggest this trend, but do not unambiguously record it.

Although to some extent AFT thermal history modelling may overestimate the amount of denudation associated with the Neogene-Quaternary event (Late Cenozoic artefactual cooling discussed earlier) the recent cooling of the Chuya-Kurai basement itself and its timing are accurately reflected. Ample independent geological and tectonic evidence, summarized in previous sections, underscores our observations. We interpret the young cooling event to be related to Late Neogene to recent denudation in a still active transpressive tectonic regime in the area. We conclude that reactivation and building of the modern Altai orogenic edifice is largely constrained to the last 15-5 Ma, or even younger as it is not completely registered in the AFT system.

Late Cenozoic cooling and denudation of Central Asia with respect to reactivation in the framework of ongoing India-Eurasia convergence was reported in AFT studies, in particular of the Tien Shan area (Hendrix et al., 1994; Sobel and Dumitru, 1997; Bullen et al. 2001). Also, closer to the collision zone, in the Altyn Tagh and the northern Tibetan Plateau, this is observed as well (e.g. Jolivet et al., 2001).

Acknowledgements

We thank F. De Corte, R. Jonckheere, and A. De Wispelaere for support during AFT analyses. J. Klerkx, L. Smirnova, and K. Theunissen are acknowledged for fieldwork and sampling assistance. This research was supported by the Fund for Scientific Research–Flanders (Belgium) where JDG is postdoctoral fellow, and by the Belgian Science Policy and the INTAS project 97-30874 (DD).

References

Allen, M.B., Vincent, S.J., 1997. Fault reactivation in the Junggar region, northwest China: the role of basement structures

during Mesozoic-Cenozoic compression. Journal of the Geological Society, London 154, 151–155.

Avouac, J.P., Tapponnier, P., 1993. Kinematic model of active deformation in Central Asia. Geophysical Research Letters 20, 895–898.

Bayasgalan, A., Jackson, J., Ritz, J.-F., Carretier, S., 1999. Forebergs, flower structures, and the development of large intracontinental strike-slip faults: the Gurvan Bogd fault system in Mongolia. Journal of Structural Geology 21, 1285–1302.

Bullen, M.E., Burbank, D.W., Garver, J.I., Abdrakhmatov, K,Ye., 2001. Late Cenozoic tectonic evolution of the northwestern Tien Shan: New age estimates for the initiation of mountain building GSA Bulletin 113, 1544–1559.

Buslov, M.M., Watanabe, T., 1996. Intrasubduction collision and its role in the evolution of an accretionary wedge: the Kurai zone of Gorny Altai (Central Asia). Russian Geology and Geophysics 37, 74–84.

Buslov, M.M., Zykin, V.S., Novikov, I.S., Delvaux, D., 1999. Cenozoic history of the Chuya depression (Gorny Altai): Structure and Geodynamics. Russian Geology and Geophysics, 40, 1687–1701.

Buslov, M.M., Saphonova, I.Yu., Watanabe, T., Obut, O.T., Fujiwara, Y., Iwata, K., Semakov, N.N., Sugai, Y., Smirnova, L.V., Kazansky, A.Yu., 2001. Evolution of the Paleo-Asian Ocean (Altai-Sayan region, Central Asia) and collision of possible Gondwana-derived terranes with the southern marginal part of the Siberian continent. Geosciences Journal 5, 203–224.

Buslov M.M., Watanabe, T., Smirnova, L.V., Fujiwara I., Iwata, K., De Grave, J., Semakov N.N., Travin, A.V., Kiryanova, A. P., Kokh, D.A., 2003. Role of strike-slip faults in Late Paleozoic-Early Mesozoic tectonics and geodynamics of the Altai-Sayan and East Kazakhstan folded zone. Russian Geology and Geophysics 44, 49–75.

Calais, E., Vergnolle, M., San'kov, V., Lukhnev, A., Miroshnitchenko, A., Amarjargal, S., Déverchère, J., 2003. GPS measurements of crustal deformation in the Baikal-Mongolia area (1994–2002): implications for current kinematics of Asia. Journal of Geophysical Research 108, 2501, doi:10.1029/2002JB002373, 13 pp.

Cunningham, D., Windley, B., Dorjnamjaa, D., Badamgarov, J., Saandar, M., 1996. A structural transect across the Mongolian western Altai: active transpressional mountain building in Central Asia. Tectonics 15, 142–156.

De Corte, F., Bellemans, F., Van den haute P., Ingelbrecht, C., Nicholl, C., 1998. A new U doped glass certified by the European Commission for the calibration of fission-track dating. In: Van den haute, P. and De Corte, F. (Eds.), Advances in fission-track geochronology, Kluwer Academic Publishers, Dordrecht, pp. 67–78.

De Grave, J., Van den haute, P., 2002. Denudation and cooling of the Lake Teletskoye region in the Altai Mountains (South Siberia) as revealed by apatite fission-track thermochronology. Tectonophysics 349, 145–159.

De Grave, J., Buslov, M.M., Van den haute, P. (accepted for publication). Distant effects of India-Eurasia convergence and intracontinental deformation in Central Asia: constraints from apatite fission-track thermochronology. Journal of Asian Earth Science.

Dehandschutter, B., Delvaux, D., Boven, A., 1997. The Lake Teletsk tectonic depression (Altai): new kinematic data and chronological relations. Annual Report of the Department of Geology and Mineralogy, Royal Museum for Central Africa, Tervuren, Belgium 1995–1996, 147–167.

Dehandschutter, B., Vysotsky, E., Delvaux, D., Klerkx, J., Buslov, M.M., Seleznev, V.S., De Batist, M., 2002. Structural evolution of the Teletsk graben (Russian Altai). Tectonophysics 351, 139–167.

Delvaux, D., Moeys, R., Stapel, G., Melnikov, A., Ermikov, V., 1995a. Paleostress reconstructions and geodynamics of the Baikal region, Central Asia, Part 1. Palaeozoic and Mesozoic pre-rift evolution. Tectonophysics 252, 61–101.

Delvaux, D., Theunissen, K., Van der Meer, R., Berzin, N., 1995b. Dynamics and paleostress of the Cenozoic Kurai-Chuya depression of Gorny Altai (South Siberia): tectonic and climatic control. Russian Geology and Geophysics 36, 26–45.

Dobretsov, N.L., Vladimirov, A.G., 2001. Continental growth in the Phanerozoic: Evidence from Central Asia. Geology, magmatism and metamorphism of the western part of Altai-Sayan Fold Region. IGCP-420, 3rd Workshop, Field Excursion Guide. Novosibirsk, pp. 139.

Dobretsov, N.L., Berzin, N.A., Buslov, M.M., Ermikov, V.D., 1995. General aspects of the evolution of the Altai region and the interrelationships between its basement pattern and the neotectonic structural development. Russian Geology and Geophysics 36, 3–15.

Dobretsov, N.L., Buslov, M.M., Delvaux, D., Berzin, N.A., Ermikov, V.D., 1996. Meso- and Cenozoic tectonics of the Central Asian mountain belt: effects of lithospheric plate interaction and mantle plumes. International Geology Review 38, 430–466.

Graham, S.A., Hendrix, M.S., Johnson, C.L., Badamgarav, D., Badarch, G., Amory, J., Porter, M., Barsbold, R., Webb, L.E., Hacker, B.R., 2001. Sedimentary record and its implications of Mesozoic rifting in southeast Mongolia. GSA Bulletin 113, 1560–1579.

Green, P.F., Duddy, I.R., Gleadow, A.J.W., Tingate, P.R., Laslett, G.M., 1986. Thermal annealing of fission tracks in apatite.1. A qualitative description. Chemical Geology (Isotopes Geoscience Section) 59, 237–253.

Hendrix, M.S., Dumitru, T.A., Graham, S.A., 1994. Late Oligocene – Early Miocene unroofing in the Chinese Tien Shan: an early effect of the India-Asia collision. Geology 22, 487–490.

Howard, J.P., Cunningham, W.D., Davies, S.J., Dijkstra, A.H., Badarch, G., 2003. The stratigraphic and structural evolution of the Dzereg Basin, western Mongolia: clastic sedimentation, transpressional faulting and basin destruction in an intraplate, intracontinental setting. Basin Research 15, 45–72.

Hurford, A.J., 1990. Standardization of fission track dating calibration: Recommendation by the Fission Track Working Group of the I.U.G.S. Subcommission on Geochronology. Chemical Geology (Isotope Geoscience Section) 80, 171–178.

Hurford, A.J., Green, P.F., 1983. The zeta age calibration of fission-track dating. Geoscience 1, 285–317.

Johnson, C.L., 2004. Polyphase evolution of the East Gobi basin: sedimentary and structural records of Mesozoic-Cenozoic intraplate deformation in Mongolia. Basin Research 16, 79–99.

Jolivet, M., Brunel, M., Seward, D., Xu, Z., Yang, J., Roger, F., Tapponnier, P., Malavieille, J., Arnaud, N., Wu, C., 2001. Mesozoic and Cenozoic tectonics of the northern edge of the Tibetan Plateau: fission-track constraints. Tectonophysics 343, 111–134.

Jonckheere, R., 2003. On the densities of etchable fission tracks in a mineral and co-irradiated external detector with reference to fission-track dating of minerals. Chemical Geology 200, 41–58.

Ketcham, R.A., Donelick, R.A., Carlson, W.D., 1999. Variability of apatite fission-track annealing kinetics: III. Extrapolation to geologic time scales. American Mineralogist 84, 1235–1255.

Ketcham, R.A., Donelick, R.A., Donelick, M.B., 2000. AFTSolve: A program for multi-kinetic modelling of apatite fission-track data. Geological Materials Research 2, 1–32.

Khain, E.V., Bibikova, E.V., Salnikova, E.B., Kröner, A., Gibsher, A.S., Didenko, A.N., Degtyarev, K.E., Fedotova, A.A., 2003. The Palaeo-Asian ocean in the Neoproterozoic and early Palaeozoic: new geochronological data and palaeotectonic reconstructions. Precambrian Research 122, 329–358.

Kravchinsky, V.A., Cogné, J.-P., Harbert, W.P., Kuzmin, M.I., 2002. Evolution of the Mongol-Okhotsk ocean as constrained by new paleomagnetic data from the Mongol-Okhotsk suture zone, Siberia. Geophysical Journal International 148, 34–57.

Laslett, G.M., Green, P.F., Duddy, I.R., Gleadow, A.J.W., 1987. Thermal annealing of fission tracks in apatite. 2. A quantitative analysis. Chemical Geology (Isotopes Geoscience Section) 65, 1–13.

Molnar, P., Tapponnier, P., 1975. Cenozoic tectonics of Asia: Effects of a continental collision. Science 189, 419–426.

Nikolaeva, T.V., Shuvalov, V.F., 1995. Mesozoic and Cenozoic evolution of surface topography in Mongolia. Geomorfologiya 2, 54–65.

Novikov, I.S., 2002. Late Paleozoic, Middle Mesozoic, and Late Cenozoic stages of the Altai orogeny. Russian Geology and Geophysics 43, 432–443.

Novikov, I.S., Delvaux, D., Agatova, A.R., 1998. Neotectonics of the Kurai ridge (Gorny-Altai). Russian Geology and Geophysics 39, 970–977.

Philip, H., Ritz, J.-F., 1999. Gigantic paleolandslides associated with active faulting along the Bogd fault (Gobi-Altay, Mongolia). Geology 27, 211–214.

Pinous, O.V., Sahagian, D.L., Shurygin, B.N., Nikitenko, B.L., 1999. High-resolution sequence stratigraphic analysis and sea-level interpretation of the middle and upper Jurassic strata of the Nyurolskaya depression and vicinity (southeastern West Siberia, Russia). Marine and Petroleum Geology 16, 245–257.

Pollitz, F., Vergnolle, M., Calais, E., 2003. Fault interaction and stress triggering of twentieth century earthquakes in Mongolia. Journal of Geophysical Research 108, 2503, doi:10.1029/2002 JB002375, 14 pp.

Şengör, A.M.C., Natal'in, B.A., Burtman, V.S., 1993. Evolution of the Altaid tectonic collage and Palaeozoic crustal growth in Eurasia. Nature 364, 299–307.

Sobel, E.R., Dumitru, T.A., 1997. Thrusting and exhumation around the margins of the western Tarim Basin during the India-Asia collision. Journal of Geophysical Research 102, 5043–5064.

Tapponnier, P., Molnar, P., 1979. Active faulting and Cenozoic tectonics of the Tien Shan, Mongolia, and Baykal regions. Journal of Geophysical Research 84 3425–3459.

Thomas, J.C., Lanza, R., Kazansky, A., Zykin, V., Semakov, N., Mitrokhin, D., Delvaux, D., 2002. Paleomagnetic study of Cenozoic sediments from the Zaisan basin (SE Kazakhstan) and the Chuya depression (Siberian Altai): tectonic implications for central Asia. Tectonophysics 351, 119–137.

Tomurtogoo, O., Windley, B.F., Kröner, A., Badarch, G., Liu, D.Y., 2005. Zircon age and occurrence of the Adaatsag ophiolite and Muron shear zone, central Mongolia: constraints on the evolution of the Mongol-Okhotsk ocean, suture and orogen. Journal of the Geological Society, London 162, 125–134.

Van den haute, P., De Corte, F., Jonckheere, R., Bellemans, F., 1998. The parameters that govern the accuracy of fission-track age determinations: a re-appraisal. In: Van den haute, P. and De Corte, F. (Eds.), Advances in fission-track geochronology, Kluwer Academic Publishers, Dordrecht, pp. 33–46.

Van der Beek, P., Delvaux, D., Andriessen, P.A.M., Levi, K.G., 1996. Early Cretaceous denudation related to convergent tectonics in the Baikal region, SE Siberia. Journal of the Geological Society London 153, 515–523.

Vergnolle, M., Pollitz, F., Calais, E., 2003. Constraints on the viscosity of the continental crust and mantle from GPS measurements and postseismic deformation models in western Mongolia. Journal of Geophysical Research 108, 2502, doi:10.1029/2002JB002374, 15 pp.

Vyssotski, A.V., Vyssotski, V.N., Nezhdanov, A.A., 2006. Evolution of the West Siberian Basin. Marine and Petroleum Geology 23, 93–126.

Wagner, G.A., Van den haute, P., 1992. Fission Track-Dating. Kluwer Academic Publishers, Dordrecht, 285 pp.

Yuan, W., Carter, A., Dong, J., Bao, Z., An, Y., Guo, Z., 2006. Mesozoic-Tertiary exhumation history of the Altai Mountains, northern Xinjiang, China: new constraints from apatite fission track data. Tectonophysics 412, 183–193.

Zorin, Yu.A., 1999. Geodynamics of the western part of the Mongolia-Okhotsk collisional belt, Trans-Baikal region (Russia) and Mongolia. Tectonophysics 306, 33–56.

Zykin, V.S., Kazansky, A.Y., 1995. Main problems of stratigraphy and paleomagnetism of Cenozoic (prequaternary) deposits in the Chuya depression of Gorno Altay. Russian Geology and Geophysics 35, 75–90.

Zykin, V.S., Lebedeva, N.K., Buslov, M.M., Marinov, V.A., 1999. The Discovery of Marine Upper Cretaceous in the Altai Mountains. Doklady Akademii Nauka, Earth Science Section, 367, 610–613.